Journal of Zhejiang University-SCIENCE A (Applied Physics & Engineering)
ISSN 1673-565X (Print); ISSN 1862-1775 (Online)
www.zju.edu.cn/jzus; www.springerlink.com
E-mail: jzus@zju.edu.cn

Performance evaluation of a micro turbo-expander for application in low-temperature solar electricity generation*

Gang PEI†, Yun-zhu LI, Jing LI, Jie JI†‡

(*Department of Thermal Science and Energy Engineering, University of Science and Technology of China, Hefei 230026, China*)

†E-mail: peigang@ustc.edu.cn; jijie@ustc.edu.cn

Received Mar. 17, 2010; Revision accepted Sept. 10, 2010; Crosschecked Jan. 25, 2011

Abstract: A micro turbo-expander capable of high working speed was specially manufactured for use in an organic Rankine cycle (ORC). A series of tests were executed to examine the performance of the machine. In the experiment, the machine was tested under different inlet pressure conditions (0.2–0.5 MPa). Data such as the compressed air pressure, temperatures of the inlet and the outlet, rotational speed, and electric power generation were analyzed to discover underlying relationships. During the test, the rotational speed of the machine reached as high as 54 000 r/min, the peak value of the temperature drop between the inlet and the outlet reached 42 °C, the maximum electric power generated by the motor-generator attached to the machine reached 630 W, and the efficiency of the machine reached 0.43.

Key words: Turbo-expander, Solar, Low-temperature, Performance evaluation
doi:10.1631/jzus.A1000105 **Document code:** A **CLC number:** TK11+4

1 Introduction

Modern society relies on fossil fuels to preserve economic growth and the standard of living. China, a large and rapidly developing country, requires equivalent energy consumption. Thus, finding a balance between the country's economy and energy requirements is essential to economic and environmental sustainability. In light of this, China has accelerated the development of its solar power, hydropower, biomass energy, and wind power to promote the use of renewable energy. In particular, the Renewable Energy Law calls for 15% of the country's energy to come from renewable sources by 2020 (NDRC, 2007).

After more than 20 years' development, solar energy generating systems have achieved great success, and gained valuable experience towards improving solar thermal energy initiatives. These solar power plants generally use the traditional steam Rankine cycle. In accordance with the steam properties of water, a steam Rankine system of economical feasibility requires an external heat source temperature above 370 °C (Hung, 2001). Thus, large areas of solar collectors with accurate tracking facilities, heat storage facilities, and complicated control systems are indispensable.

Solar energy is characterized by strong dispersion and low-density of energy flow, while organic fluids possess high pressure at a low boiling point. In an organic Rankine cycle (ORC), an organic medium is used as the working substance instead of water. With the ORC process, it is possible to turn any kind of low-temperature heat source efficiently into electricity.

Research has been conducted to demonstrate the technical and economical feasibility of the ORC in generating electricity from low-temperature sources such as geothermal sources, solar energy, waste heat of industrial processes, and biomass combustion.

‡ Corresponding author
* Project (Nos. 50974150 and 50708105) supported by the National Natural Science Foundation of China

Tchanche *et al.* (2009) discussed the influence of organic fluids (such as R134a, R245fa, and R600) on the ORC. Mago and Chamra (2008) analyzed the ORC system through a novel approach called exergy-topological method.

Usually, heat at relatively low temperatures is rejected as waste in industrial processes, which can be used as a heat source. For example, Engin and Ari (2005) showed that 40% of the heat used in the cement industry was discharged as waste flue gases, whose temperature varies between 215 and 315 °C. There is great market potential for the ORC technology in this field. Chacartegui *et al.* (2009) described a project that aimed at capturing waste heat from a commercial gas turbine to generate electricity by the ORC.

The range of the temperatures of geothermal heat sources is large. The lowest temperature for the ORC heat recovery is approximately 100 °C, while other ORC geothermal power plants work at a temperature reaching over 200 °C. Higher temperature (>150 °C) geothermal heat sources make combining heat and power generation possible. The condensing temperature is adjusted to a higher temperature (e.g., 60 °C), allowing cooling water to be used for heating. The global energy efficiency is therefore increased, at the cost of the electrical efficiency. Dipippo (2004) introduced two pilot binary geothermal power plants built in Japan. These plants use R114 and isobutane as the working fluids respectively, and both had a rated power of 1000 kW in 1978. Saleh *et al.* (2007) discussed two geothermal power plants in Altheim, Austria, and Neustadt-Glewe, Germany. Both of the plants use n-perfluoropentane as a working fluid. Franco and Villani (2009) investigated the exploitation of geothermal energy by ORC, and provided optimized schemes.

Biomass is now a major resource in the renewable energy field. It is abundant in agricultural and industrial processes, and is friendly to the environment. Drescher and Bruggemann (2007) studied the ORC applied to biomass power. Dong *et al.* (2009) focused on an application that combined the ORC with a biomass-fuelled combined heat and power (CHP) system.

Combining solar thermal collectors with the ORC system, electricity from relatively low-temperature solar thermal sources can be efficiently generated. In turn, the ORC system has both lower collector temperature and higher collecting efficiency (reduced ambient losses), allowing for the possibility of reducing the size of the solar field. In 2005, a 250 kW prototype ORC plant was built by GMK, Germany. The plant aims at simulating a solar system, and uses a natural gas boiler as a heat source. The electrical efficiency of the plant was about 15 % (Quoilin and Lemort, 2009).

Fig. 1 shows a typical solar-ORC electrical process. First, the heat transfer fluid (HTF) is heated in the solar fields, where the solar energy is concentrated. The high-temperature HTF is then pumped into a heat exchanger, where the organic working fluid is vaporized at a high pressure. The organic vapor runs the turbine, transforming the internal energy into the mechanical energy. The vaporized working liquid from the turbine is processed by the condenser, and recondensed into the liquid form. Finally, the liquid is pumped to a reservoir tank before ultimately re-entering the heat exchanger, where the system cycle begins again.

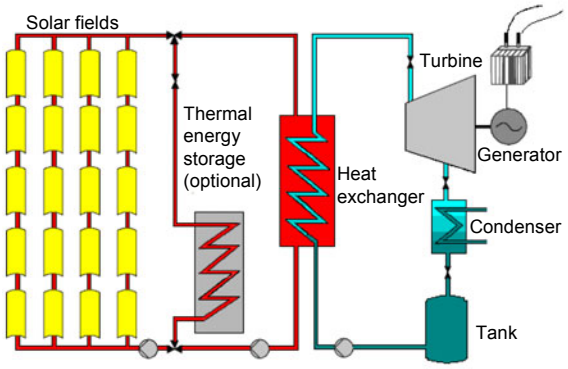

Fig. 1 Solar-organic Rankine cycle system sketch

Kane *et al.* (2003) introduced a concept of a mini-hybrid solar power plant integrating solar concentrators, two superposed ORCs, and a bio-diesel engine to meet the pumping, cooling, and electricity needs of remote settlements. In Arizona in 2006, a 1 MW concentrated solar power (CSP) plant working with ORC was established. This system uses *n*-pentane as the working fluid, and Ormat Technologies Inc. provided the ORC module. The solar to electricity efficiency is 12.1 % on the design point (Canada *et al.*, 2004).

The solar-ORC electric system has the following advantages.

1. The system has minimal requirements in terms of heat source temperature (80–200 °C), collector devices, and solar tracking equipment. This means low construction costs and ease in large-scale utilization.

2. The system requires smaller solar field areas, allowing it to be integrated into buildings (and other structures) to serve as heating and cooling mechanisms. Forming a system that integrates the solar-ORC electricity system with the heating and cooling system of the building, thus increasing its utilization, is possible.

2 Test platform

The expanders are the key parts of the ORC systems. The selection of the expander machine strongly depends on the operating conditions and the size of the system. Two main types of expanders can be distinguished, the turbo and the positive displacement types.

Similar to refrigeration applications, positive displacement expanders such as scroll expanders are more appropriate to small-scale ORC units, because they are characterized by lower flow rate, higher pressure ratios, and much lower rotational speeds than turbo-machines (Persson, 1990). Currently, most of the positive displacement expanders employed in ORC units are obtained by modifying existing corresponding compressors. Yanagisawa *et al.* (2001) converted an oil-free scroll air compressor to an oil-free scroll type air expander, and performance of the machine was investigated theoretically and experimentally. Zanelli and Favrat (1994) described a scroll expander generator modified from a standard hermetic compressor, and employed the machine as the engine in an ORC system.

Turbo-expanders are mainly designed for large-scale applications, and show a high degree of technical maturity. There are now mature products available on market; e.g., the company Infinity Turbine provides radial turbo-expanders in the ORC solution.

A micro radial-axial turbo-expander is used in this experiment. For this kind of expander, the blades within the chamber are located radially, pointing to the radial direction near the nozzle entrance and gradually turning to the axial direction. This design guarantees the expander shaft rotation and smooth movement of the vapor in the chamber. The radial-axial turbo-expander has many advantages, such as compact structure for easy manufacture, simplex-type lightweight construction, high efficiency, and a single-stage expansion rate that indicates a big enthalpy drop, amongst others. For these reasons, the radial-axial turbo-expander is widely used in places with small flow and low power. For example, the expander's cooling effect is commonly used in the air-conditioning systems of airplanes and in common cooling of cryogenic devices on the ground. It can also provide power sources for the supercharging of internal combustion engines and auxiliary equipment on ships and aircraft.

Fig. 2 shows the turbo-expander used in the experiment, of which the outline dimensions are 252.6 mm×138 mm×237 mm, the inlet diameter is 22 mm, and the outlet diameter is 32 mm.

Fig. 2 Turbo-expander used in the experiment

High-pressure gas expands and accelerates after being injected into the expander. This will move the radial bladed impeller, causing the vapor temperature to drop. Consequently, the internal energy of the hot vapor is transformed into the mechanical energy, and finally—if a generator is assembled—into electricity. The rotational speed of the expander in the experiment can reach 60000 r/min. A reduction gear between the expander and the generator is also necessary to ensure the generator to run at 3000 r/min.

The decision to use compressed air to simulate organic fluids in our experiment is based on the following considerations.

1. Compressed air will maintain its gaseous state without phase transition. Since liquid droplets will significantly disrupt the turbo-expander blades when the spinning speed is very high, compressed air, which can be approximately recognized as ideal gas, will protect the turbo-expander in the test.

2. Research on the performance of compressed air is also of practical significance. In industrial processes, such as those in cement factories, chemical plants, metallurgical industries, and paper mills, a great amount of residual pressure energy is generated as a by-product. Compressed air will simulate the utilization of these pressure sources that are usually disposed of as waste energy.

Fig. 3 illustrates the main components of the experiment platform. The generator is connected to the turbo-expander via a gearbox, which reduces the rotational speed of the turbo-expander. The axial rotation drives the generator to produce electrical power. The lower inertia of the turbo-expander generator shaft allows it to attain a high rotational speed easily, as fast as 60000 r/min. Consequently, the turbo-expander employs a gearbox to diminish the rotational speed and to match the power generator. The generator (8SC3110VC, Prestolite Electric Beijing Ltd., China) used in this study is a commercial product used in motorbuses. The generated current is consumed by a series of direct current (DC) bulbs (24 V) also used in motorbuses. The quantity of the generated power can be calculated by measuring the electricity voltage and the current. The generator loads can be adjusted by changing the number of bulbs.

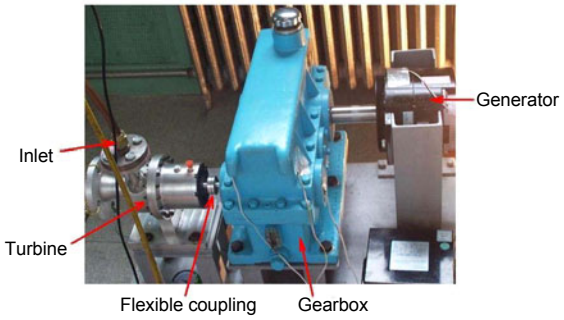

Fig. 3 Experiment setup

Incoming pressure and flow rate in the turbo-expander can be regulated manually by a valve set between the compressed air tank and the turbo-expander. A flow meter is set before the valve to measure and to record the volume flow rate of the compressed air. In this study, a LWGY-turbine flow meter (Pope Hefei Instrument Co., Ltd., China) was used. The rotational speed of the machine was obtained by measuring the alternating current (AC) frequency of the generator before its rectification.

K-type chromel (chromium-nickel alloy) alumel (aluminum-nickel alloy) thermocouples were used to measure temperatures within the range of −200 to 1370 °C, with an accuracy of ±2.2 °C or 0.75 % of the measurement. Temperatures at the turbo-expander inlet and outlet, and the ambient temperature were measured using this kind of thermocouple. A ceramic pressure transmitter (506, Huba Control Co., Switzerland), ranging from 0 to 4 MPa with an accuracy of ±1.0 %, was used to measure the pressure.

All measurement data were recorded and stored on disk via the computer data-acquisition system Agilent Bench Link Data Logger (34970A, Agilent Technologies, US). With the above experimental setup, the corresponding testing procedure is given in the following section. Fig. 4 shows the schematic view of the testing platform, consisting of the turbo-expander, gearbox, and generator, fixed on a heavy steel test bed.

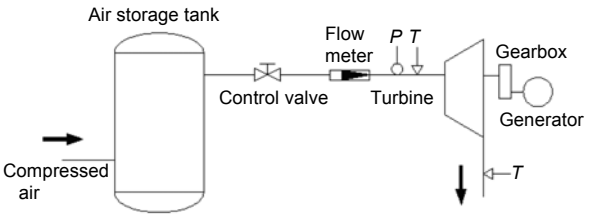

Fig. 4 View of the testing platform
P: pressure; *T*: temperature

After the compressed air is released from the storage tank, a flow meter located between the valve and the machine records the vapor flow rate within the pipe. Air temperature and pressure are monitored at the entrance nozzle of the turbo-expander. When the vapor is discharged to the ambient environment directly, its pressure is shown to be equal to the environmental atmosphere. Therefore, only the temperature measuring point is recorded at the turbo-expander exit.

During the experiment, gas pressure at the expander entrance was recorded as 0.2, 0.3, 0.4, and 0.5 MPa. Under each pressure condition, different numbers of bulbs were lit to adjust the electrical load

of the generator. During these two sets of adjustments (pressure and electrical load), data on the rotor speed, gas input pressure, air flow rate, and temperature of output air were gathered in order to analyze the underlying relations between these parameters.

3 Results and analysis

In order to characterize the operation of the expander, a series of experimental tests were carried out, and the recorded data were analyzed.

Fig. 5 shows the curves of the inlet pressure and the rotational speed versus time, when the generator load is unchanged by maintaining the number of bulbs. It shows that the changes of the rotational speed lag behind the pressure; that is, the speed rises when the inlet pressure increases. Since the high-speed turbo-expander is the core piece of equipment of the system, its stability is affected by many internal and external factors under high-speed condition, with the inlet pressure being the decisive factor.

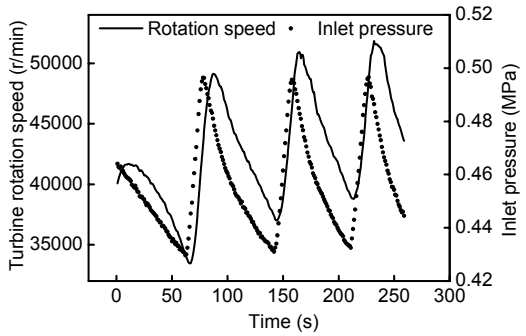

Fig. 5 Inlet pressure and rotational speed versus time

Fig. 6 shows the relationships between the expander's flow rate, rotational speed, and the inlet pressure. Obviously, the mass flow rate increased with the increase of the expander's rotational speed. With the inlet pressure fixed at 0.5 MPa, when rotational speed is 27 000 r/min, the mass flow rate is 590 kg/h; when the rotational speed is 52 000 r/min, the flow rate increases to approximately 690 kg/h. The mass flow rate increased while the expander's inlet pressure ascended. When the machine ran at 40 000 r/min, the mass flow rates varied, being 246, 532, and 606 kg/h, respectively, with different inlet pressures (0.3, 0.4, and 0.5 MPa).

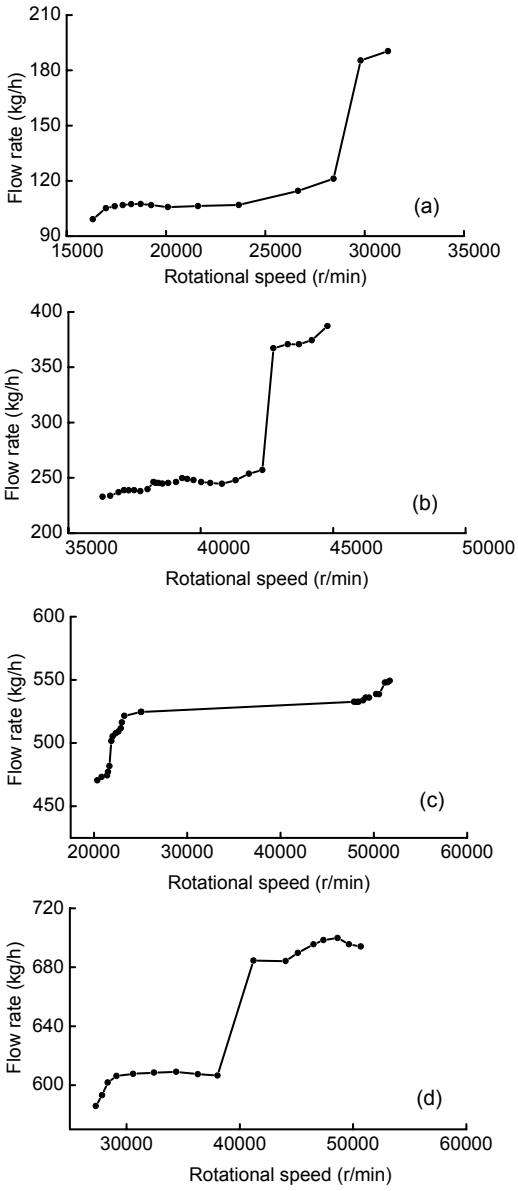

Fig. 6 Flow rate versus the rotational speed under various pressures

(a) 0.2 MPa; (b) 0.3 MPa; (c) 0.4 MPa; (d) 0.5 MPa

Data shows that the temperature drop between the machine inlet and the outlet increases with shaft speed (Fig. 7). When run at the rotational speed of 53 000 r/min, the temperature drop reached 43 °C. This means that in a higher rotational speed condition, the machine increases the energy conversion: more internal energy of the compressed air is converted to the mechanical energy of the shaft. During the test, the ambient temperature was stable and kept at 30 °C.

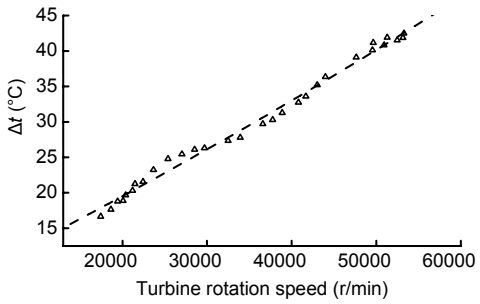

Fig. 7 Temperature drop versus the rotational speed with the inlet presure of 0.4 MPa

While keeping the inlet pressure fixed at 0.5 MPa, adjustments of the shaft speed influence the enthalpy drop and power generation. The relationships among them are shown in Fig. 8.

The rotational speed was adjusted by changing the number of the light bulbs. For simplicity and clarity, the number of the bulbs is not displayed in Fig. 8. The enthalpy drop increased as the speed of the shaft ascended, showing a different tendency from that of the electric power generation. The electric power increased as the rotational speed increased at first, and reached the peak value (around 620 W) at 30000–42000 r/min. From this point on, the electric power decreased despite the increase in the rotational speed. Power generation is affected by many factors, including a series of energy transmissions as well as energy losses that take place in the turbo-expander, reduction gear, and the generator before the electricity is generated. A higher rotational speed brings a larger enthalpy drop, meaning a larger proportion of the internal energy is converted to the mechanical energy. In addition, it produces lower efficiency and a higher energy loss to the reduction gear.

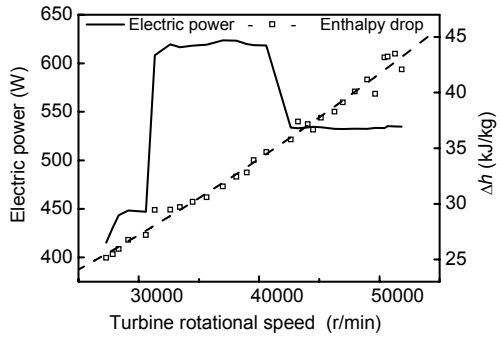

Fig. 8 Electric power and enthalpy drop versus the rotational speed

Keeping the inlet pressure fixed at 0.5 and 0.4 MPa, the rotational speed of the machine changed while modifying the loads. Turbine efficiency η is defined in (Qi, 1992) as

$$\eta=\Delta h/\Delta h_s, \tag{1}$$

where Δh is the actual enthalpy drop in the machine, and Δh_s is the isentropic enthalpy drop.

Given the pressure and temperature, the corresponding Δh and Δh_s can be calculated. The machine efficiency versus the rotational speed is shown in Fig. 9.

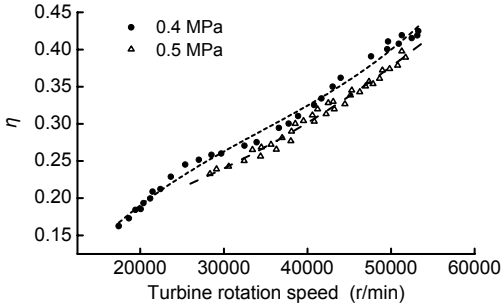

Fig. 9 Efficiency versus the rotational speed

Under the design conditions, higher speed means higher efficiency. Keeping the inlet pressure stable at 0.4 MPa, when the rotational speed was 20000 r/min, the efficiency was approximately 0.19. When the rotational speed increased to 53000 r/min, the efficiency increased to approximately 0.42.

Fig. 9 clarifies that the relationship between the speed and the efficiency is linear. When the inlet pressure of the turbo-expander shifted to 0.5 MPa, the dynamic relationship between the rotational speed and the efficiency shows the same trend.

4 Conclusions

The following are the conclusions.

1. The inlet pressure is the decisive factor affecting the rotational speed and the mass flow rate. When the inlet pressure increases, the rotational speed and the mass flow rate increase accordingly.

2. The rotational speed is the decisive factor affecting the temperature drop, enthalpy drop, and efficiency. As the rotational speed increases, the parameters mentioned above rise accordingly.

3. The electric power generation has the following relationship with the machine speed. Initially, the electric power increases as the rotational speed increases, reaching a peak value at 30 000–42 000 r/min. From then on, despite an increase in the rotational speed, the electric power decreases. Energy losses in the reduction gear, which rise significantly as the speed increases gradually, can account for this.

References

Canada, S., Cohen, G., Cable, R., Brosseau, D., Price, H., 2004. Parabolic Trough Organic Rankine Cycle Solar Power Plant, NREL/CP-550-37077. DOE Solar Energy Technologies Program Review Meeting, Denver, USA.

Chacartegui, R., Sanchez, D., Munoz, J.M., Sanchez, T., 2009. Alternative ORC bottoming cycles for combined cycle power plants. *Applied Energy*, **86**(10):2162-2170. [doi:10.1016/j.apenergy.2009.02.016]

Dipippo, R., 2004. Second law assessment of binary plants generating power from low-temperature geothermal fluids. *Geothermics*, **33**(5):565-586. [doi:10.1016/j.geothermics.2003.10.003]

Dong, L.L., Liu, H., Riffat, S., 2009. Development of small-scale and micro-scale biomass-fuelled CHP systems—a literature review. *Applied Thermal Engineering*, **29**(11-12):2119-2126. [doi:10.1016/j.applthermaleng.2008.12.004]

Drescher, U., Bruggemann, D., 2007. Fluid selection for the organic Rankine cycle (ORC) in biomass power and heat plants. *Applied Thermal Engineering*, **27**(1):223-228. [doi:10.1016/j.applthermaleng.2006.04.024]

Engin, T., Ari, V., 2005. Energy auditing and recovery for dry type cement rotary kiln systems—a case study. *Energy Conversion and Management*, **46**(4):551–562. [doi:10.1016/j.enconman.2004.04.007]

Franco, A., Villani, M., 2009. Optimal design of binary cycle power plants for water-dominated, medium-temperature geothermal fields. *Geothermics*, **38**(4):379-391. [doi:10.1016/j.geothermics.2009.08.001]

Hung, T.C., 2001. Waste heat recovery of organic Rankine cycle using dry fluids. *Energy Conversion and Management*, **42**(5):539-553. [doi:10.1016/S0196-8904(00)00081-9]

Kane, M., Larrain, D., Favrat, D., Allani, Y., 2003. Small hybrid solar power system. *Energy*, **28**(14):1427-1443. [doi:10.1016/S0360-5442(03)00127-0]

Mago, P.J., Chamra, L.M., 2008. Exergy analysis of a combined engine-organic Rankine cycle configuration. *Proceedings of the Institution of Mechanical Engineers, Part A-Journal of Power and Energy*, **222**(8):761-770. [doi:10.1243/09576509JPE642]

NDRC (National Development and Reform Commission), 2007. The National Long-Term Plan of the Development of the Renewable Energy. NDRC, Beijing, China, p.18- 19 (in Chinese).

Persson, J.G., 1990. Performance Mapping vs Design Parameters for Screw Compressors and other Displacement Compressor Types. VDI Berichte, nr. 859, Düsseldorf, Germany.

Qi, M., 1992. Refrigeration Accessories. Aviation Industry Press, Beijing, p.28-30 (in Chinese).

Quoilin, S., Lemort, V., 2009. Technological and Economical Survey of Organic Rankine Cycle Systems. European Conference on Economics and Management of Energy in Industry, Vilamoura, Portugal.

Saleh, B., Koglbauer, G., Wendland, M., Fischer, J., 2007. Working fluids for low-temperature organic Rankine cycles. *Energy*, **32**(7):1210-1221. [doi:10.1016/j.energy.2006.07.001]

Tchanche, B.F., Papadakis, G., Lambrinos, G., Frangoudakis, A., 2009. Fluid selection for a low-temperature solar organic Rankine cycle. *Applied Thermal Engineering*, **29**(11-12):2468-2476. [doi:10.1016/j.applthermaleng.2008.12.025]

Yanagisawa, T., Fukuta, M., Ogi, Y., Hikichi, T., 2001. Performance of an Oil-Free Scroll-Type Air Expander. Proceedings of the IMECHE Conference Transactions on Compressors and Their Systems, London, UK, p.167-174.

Zanelli, R., Favrat, D., 1994. Experimental Investigation of a Hermetic Scroll Expander-Generator. Proceedings 12th Internnational Compressor Engineering Conference, Purdue, USA, p.459-464.